JOURNAL of
MATERIALS and MECHATRONICS:A

e-ISSN 2717-8811
JournalMM, 2023, 4(2), 588-597
https://doi.org/10.55546/jmm.1388504

Araştırma Makalesi / Research Article

Effect of Welding Methods and Compound Reinforcement Used in Joining Natural Gas Pipes on Weld Strength

Rıza KARA[1*], Fatih ÇOLAK[2], Gökhan YILDIRIM[3], Hakan Furkan AKSU[4]

[1] Uşak Üniversitesi, Teknik Bilimler Meslek Yüksekokulu, Makine ve Metal Teknolojileri Bölümü, Uşak, Türkiye,
ORCID ID: https://orcid.org/0000-0002-0820-2577, riza.kara@usak.edu.tr
[2] Uşak Üniversitesi, Teknik Bilimler Meslek Yüksekokulu, Makine ve Metal Teknolojileri Bölümü, Uşak, Türkiye,
ORCID ID: https://orcid.org/0000-0002-1161-9875, fatih.colak@usak.edu.tr
[3] Uşak Üniversitesi, Teknik Bilimler Meslek Yüksekokulu, Makine ve Metal Teknolojileri Bölümü, Uşak, Türkiye,
ORCID ID: https://orcid.org/0000-0002-6863-171X, gokhan.yildirim@usak.edu.tr
[4] Nuri Şeker Uşak Şeker Fabrikası, Uşak, Türkiye,
ORCID ID: https://orcid.org/0009-0006-1521-2702, hakanfurkan_123@hotmail.com

Geliş/ Received: 09.11.2023; **Kabul / Accepted:** 21.12.2023

ABSTRACT: In this study, API 5L X52 steel pipe with a diameter of 1/2 inch and a thickness of 2.8 mm was cut into a 100 mm length and the weld grooves were machined for the weldability with different welding processes using SiC additions. The steel pipes were welded with welding methods of oxy-gas, electric arc and MAG. The specimens were welded in two ways: with and without silicon carbide (SiC) reinforcement. The welded samples were prepared for microstructure, tensile, fatigue and hardness tests in accordance with the standards and mechanical tests were applied. The highest yield strength was obtained with the electric arc welded sample using a rutile electrode with SiC reinforcement. It was observed that the mechanical properties of API 5L X52 steel welds were improved with the addition of SiC reinforced.

Keywords: API 5L X52 steel, Welding methods, Mechanical properties, SiC

*Sorumlu yazar / Corresponding author: riza.kara@usak.edu.tr

Bu makaleye atıf yapmak için /To cite this article

Kara, R., Çolak, F., Yıldırım, G., Aksu, H.F. (2023). Effect of Welding Methods and Compound Reinforcement Used in Joining Natural Gas Pipes on Weld Strength. Journal of Materials and Mechatronics: A (JournalMM), 4(2), 588-597.

1. INTRODUCTION

Natural gas, which has a wide area of use in the world, is the most consumed fuel (Biresselioglu et al., 2015). Safety and economy should be taken into consideration in the selection of natural gas pipes to be used for transporting the natural gas from its source (Capelle et al., 2013). Pipelines are the most common method in the world to transport high-consumption and constantly used liquids and gases over long distances, such as oil, water, and natural gas (Abedi et al., 2007; Baek et al., 2010; Javidi et al., 2014). Today, these pipes are preferred because they are easy to join by welding, are safe and economical (Mulder et al., 2007).

X52 type steel pipes are one of the preferred materials used for the transmission of liquid and gaseous fuels (Ju et al., 2003). X52 type steels constitute an important steel group preferred due to their high yield strength and high toughness properties. Conventional arc welding methods are widely used in joining of structural steels including stainless grades (Ezer & Cam, 2022; Senol & Cam, 2023; Serindag & Cam, 2021; Serindag & Cam, 2022; Serindag & Cam, 2023; Serindag et al., 2022a; Serindag et al., 2022b). However, the most obvious problem encountered during welding in these steels is the tendency for hardening that occurs in the heat affected zone (HAZ) (Seyedrezai et al., 2014). Micro islands consisting of martensite and austenite containing high carbon may form in the HAZ of these steels (Bhadeshia et al., 2004; Bohemen et al., 2017; Hossain et al., 2017). The amount of this micro-sized island is directly affected by the cooling rate. The effect of microalloying elements such as titanium (Ti) and boron (B) on the toughness of HAZ is related to the carbon equivalent value of X52 type steels. The carbon equivalence of X52 type steels is in the appropriate range for good toughness in the HAZ (Handoko et al., 2019). High amounts of silicon (Si) are harmful for welding. However, when the manganese rate is increased, the amount of Si can also be increased. In fusion welds of steels containing more than 0.7% Si, if necessary, precautions are not taken, it occurs as a pore and crack defect in the silicon oxide welded area (Ghosh et al., 2013; Jonas et al., 2013). The presence of Mg in the filler metal can provide useful properties through alloying (Jayashree et al., 2020).

However, in traditional welding processes, differences occur in the physical properties of the weld metal and the reinforcement phase due to welding defects such as slag, porosity and recovery of SiC particles in the melting weld zone. Thus, a brittle phase forms due to chemical reactions occurring at high temperatures between the weld metal and the reinforcement phase, making high-quality weld joint difficult (Jayashree et al., 2021). Therefore, lower Si content in SiC reinforced composites negatively affects the desired results after welding (Iseki et al., 1984).

In this study, the welding of API 5L X52 steel were investigated using oxy-gas, electric arc welding, MAG welding methods with and without SiC reinforcement. These welding processes were performed using different welding methods, and as a result, tensile and fatigue strengths and hardness distributions were calculated. The microstructure-mechanical property relationship of welded samples was determined through tensile, fatigue and hardness testing.

2. MATERIALS AND METHODS

The materials and methods used in the experimental methods for experimental studies are given below. The chemical composition analysis (% weight) of X52 steel pipe used for welding is given in Table 1, and its mechanical properties are given in Table 2. At the same time, the ferrite and perlite ratios of the X52 steel pipe are given in Table 3.

Table 1. Chemical Composition Analysis (% Weight) Results of X52 Steel Pipe

	C	Mn	Si	Cu	Al	Nb	S	P	V	Cr
X52	0,106	0,91	0,24	0,021	0,039	0,02	0,007	0,013	0,002	0,017

Table 2. Mechanical Properties of X52 Steel Pipe (API specification 5L, 2018)

	0.2% offset yield strength, MPa	Tensile strength, MPa
X52	360 (min)	460 (min)

Table 3. Ferrite to Perlite Ratios of X52 Steel Type (Tobón et al., 2014)

Steel Type	Ferrite Ratio	Perlite Ratio
X52	86,64	13,35

In this study, X52 pipes of 1/2 inch diameter, 2.8 mm thick and 100 mm long were welded using Oxy-gas, Electric Arc and MAG welding methods. Table 4 shows the weld parameters of all four weld methods and conditions for SiC reinforcement used for the welding of X52 pipe steels.

Table 4. Prepared Samples and Welding Conditions

	Weld	Addition	Comp.	Current(A)		Weld	Addition	Compound	Current(A)
1	Oxy-gas	∅ 2 mm AISI 1020 Steel	---	---	**5**	Oxy-gas	∅ 2 mm AISI 1020 Steel	2gr Cellulosic Varnish + 2 gr SiC	---
2	EAW	∅ 3,25 Rutile (E-6013)		115	**6**	EAW	∅ 3,25 Rutile (E-6013)		115
3	EAW	∅ 3,25 Cellulosic (E8010-G)		115	**7**	EAW	∅ 3,25 Cellulosic (E8010-G)		115
4	MAG	∅ 1 mm Steel (SG2)		125	**8**	MAG	∅ 1 mm Steel (SG2)		125

Samples 1 and 5 were welded in a single pass with oxy-gas (Oxy-Acetylene) welding (Fig. 1a). Samples 2, 3, 6 and 7 were tack welded from four different locations and then welded in a single pass using electric arc welding at 115 A. MAG welding of samples 4 and 8 was done with pure CO_2 (100%) gas (Fig. 1b). First, the samples were tack welded from four different locations and then welded in a single pass with 125 A and 1.5 m/s wire feed speed. For samples 5, 6, 7 and 8, a mixture of cellulosic varnish (2 g) and SiC (2 g) was prepared and applied to the weld joints.

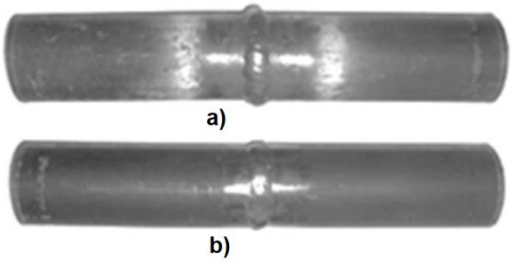

Figure 1. Welded X52 steel pipe

Transverse tensile samples were prepared from the welded samples according to TS EN ISO 4136 standard. Tensile test results were obtained with 3 test samples at room temperature and under each condition, by selecting 2 mm/min as the tensile speed. Hardness values from the welding areas of the samples welded by different welding methods were measured in Rockwell A (HRA). In metallographic examinations, the welded parts were cut and ground perpendicular to the direction of welding progress. The polished samples were etched with 3% Nital + alcohol mixture. During metallographic examinations, images were taken with a microscope at 100X and 200X magnifications.

3. RESULTS AND DISCUSSION

The results of the tensile tests of the welded samples with and without SiC addition are shown in Figure 2. As can be seen, the highest yield strength of 380 MPa was measured in the samples welded with electric arc welding using rutile and electrode with an addition of SiC. It is seen that SiC reinforcement has an effect on the yield strength and maximum tensile strength when the welds made with all welding methods are compared. In welding processes without SiC reinforcement, the yield strength was obtained as 90 MPa in samples welded with oxy-gas, 95 MPa in EAW samples made with rutile electrode, and 70 MPa in samples welded using cellulosic electrode. The yield strength of the samples welded with the MAG welding method was obtained as 160 MPa. In the samples welded using oxy-gas, electric arc and MAG welding methods without SiC reinforcement, the highest tensile strength was obtained as 313 MPa in the sample joined by the MAG welding method. The lowest tensile strength was obtained at 215 MPa in the sample welded with oxy-gas welding. The highest % elongation value was obtained as 14.7% in the SiC unreinforced welded sample joined by the EAW method with rutile electrodes. The lowest % elongation was obtained as 3.5% in the sample joined with MAG welding without SiC reinforcement. The difference in these two tensile strength and % elongation amounts is due to the difference in the amount of ferrite formed in the microstructure of the welded joints.

The yield strength of SiC reinforced welds was obtained as 340 MPa in samples welded with oxy-gas welding method, 380 MPa in samples welded with EAW, and 200 MPa in samples welded with MAG welding method. Vargas-Arista et al., 2012, in their study, stated that the yield strength was 420-520 MPa in samples joined using submerged arc welding. In another study (Candan et al., 2006), it was stated that the highest values were obtained in the welding of X52 steel pipes with the MAG welding method.

The maximum % elongation in welded specimens were 15.5% in samples welded with oxy-gas with SiC reinforcement, 16% in samples welded with EAW with rutile electrode, 17.5% with cellulosic electrode and 4.25% in MAG welding. When the tensile test results are examined, the values closest to the yield limit of the main material, which is approximately 360 MPa (Table 2), were obtained in SiC reinforced samples. The yield stress in the SiC reinforced EAW sample was obtained higher than that of the main material (380 MPa). The yield strength of the samples joined by welding without the use of reinforcement was lower than the yield strength of the base material. Regarding the tensile strength of the samples welded by SiC reinforced oxy-gas, electric arc and MAG welding methods, the highest tensile strength was obtained as 544 MPa in the sample joined by the rutile electrode EAW method, and the lowest tensile strength was obtained as 329 MPa in the sample joined by the MAG welding method. The highest average % elongation of the SiC reinforced welded samples was obtained as 17.5% in the sample joined by the cellulose electrode EAW method. The

lowest % elongation value was obtained as 4.25% in the sample joined with SiC reinforced MAG welding. The results of the fatigue test performed are given in Table 5.

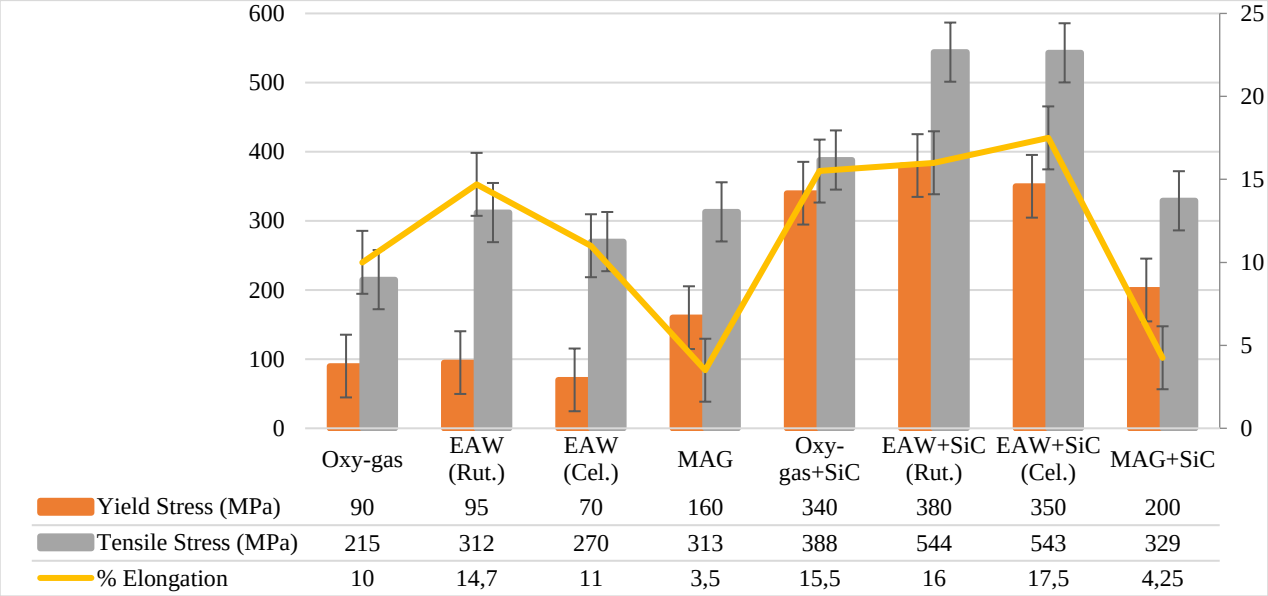

Figure 2. Tensile test results graph

Table 5. Fatigue Test Results

No	1	2	3	4	5	6	7	8
Number of Cycles	1000	1291	3700	26298	60000	52000	27648	27740
Fracture Zone	W.Z.	W.Z.	W.Z.	HAZ	B.M.	W.Z.	W.Z.	HAZ

When the fatigue test results of welds without SiC reinforcement were examined, the longest number of cycles was seen in the sample 4 that was joined using MAG welding method. The lowest number of cycles was obtained in the oxy-gas welded sample. Except for the sample joined with the MAG welding method, it was observed that there were ruptures in the weld area in the samples welded with other welding methods.

However, the rupture occurred in the HAZ region of the sample welded with the MAG welding method. The Mn and C content of the additional wire used here affected the tensile and fatigue test results in the welded samples. This effect was observed clearly in the MAG welding method. In microstructure studies, changes in the properties of the electrodes used have led to changes in the weld microstructures.

When the fatigue results were examined, the longest number of cycles in the samples welded with SiC reinforcement was obtained in the welding process with oxy-gas welding (sample no. 5). The lowest number of cycles was seen in sample number 8, which was welded by the MAG welding method with SiC reinforcement. The hardness of the weld areas of the welds was also measured. To compare the hardness results of each weld, first the hardness of the base material and then the welded samples were measured. The hardness values obtained here are given in Table 6.

In a study (Candan et al., 2006), micro hardness values of X52 steel pipes were obtained as 155-160 HV5 in samples welded in horizontal groove position with the MAG welding method. The hardness value was higher as a result of welding with the MAG welding method compared to the main material and oxy-gas welding method. It was observed that the 66.2 HRA value obtained in

experimental studies was approximately 318 HV from the hardness conversion table. This can be explained by the fact that the SiC reinforcement breaks down due to the high temperature generated by welding electrode during the welding process, creating carbon-rich regions in the weld metal structure.

Table 6. Hardness Values

No	B.M.	1	2	3	4	5	6	7	8
Hardness (HRA)	23,2	22,5	40,6	41,8	40,7	43,3	44,7	56,4	66,2

The samples were examined metallographically to determine the microstructure-mechanical property relationship. The microstructure of the base material is given in Figure 3. Separate optical microstructure images were taken from the HAZ and weld metal of the welded samples. When the overall microstructures were examined, it was observed that the needle structures seen were acicular ferrite. The rapid solidification of the samples after welding explains the reason for the formation of this acicular ferrite structure.

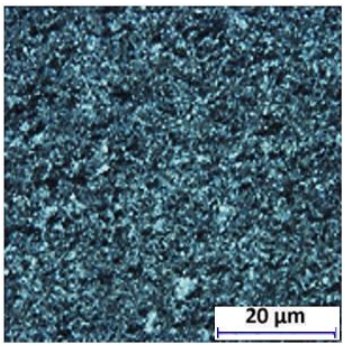

Figure 3. Microstructure of base material

The microstructure of the samples welded with oxy-gas welding method is given in Figure 4 (a), the weld metal without SiC reinforcement, the HAZ with SiC reinforcement in Figure 4 (b), and the weld metal with SiC reinforcement in Figure 4 (c). Here, it is observed that after the oxy-gas welding, the grain size of the sample becomes larger compared to the base metal.

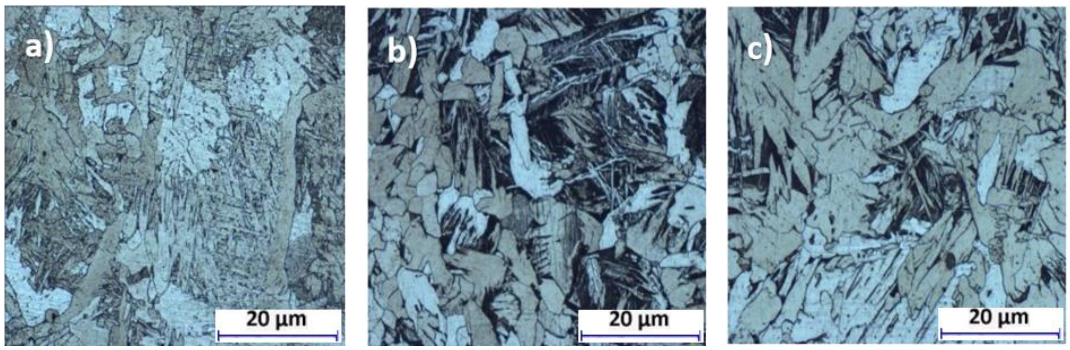

Figure 4. Microstructure of samples welded by oxy-gas welding method (100X) (a) SiC without, weld metal, (b) SiC reinforced, HAZ, (c) SiC reinforced weld metal microstructure

The SiC-reinforced weld metal of the sample welded using EAW with a rutile electrode is shown in Figure 5 (a), the SiC reinforced HAZ is shown in Figure 5 (b), and the microstructure of the

SiC reinforced weld metal is shown in Figure 5 (c). The microstructure obtained with the SiC reinforcement appears to be coarsened. The phases in the intergranular region also appers darker due to refinement of local microstructure. It is also possible that the decomposition of SiC and hence the addition of Si and C into weld metal increased the amount of residual phase that appear as dark region due to increased activity of alloying elements insoluble in ferrite phase. Thus, with slow cooling, both the grains and the carbides in the intergranular region became larger. The SiC-reinforced weld metal of the sample welded using EAW with cellulosic coated electrode is shown in Figure 6 (a) and (b), the SiC reinforced HAZ, and the microstructure of the SiC reinforced weld metal is shown in Figure 6 (c).

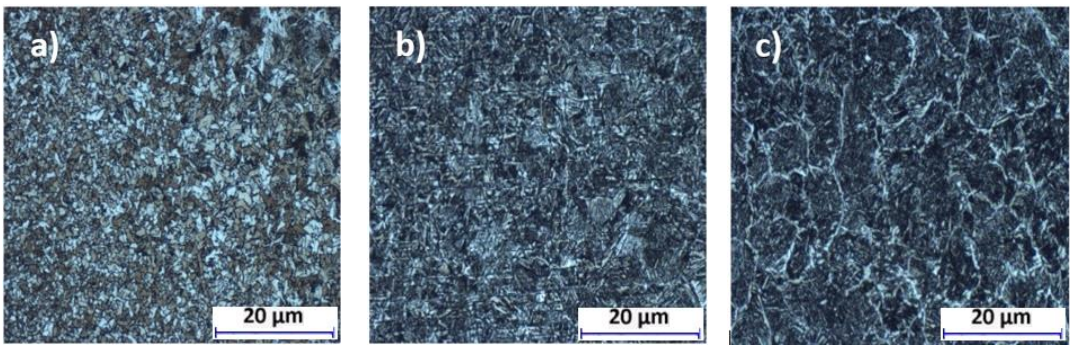

Figure 5. Microstructure of the sample welded using rutile electrode by electric arc welding method (100X) (a) SiC without, weld metal, (b) SiC reinforced, HAZ, (c) SiC reinforced weld metal microstructure

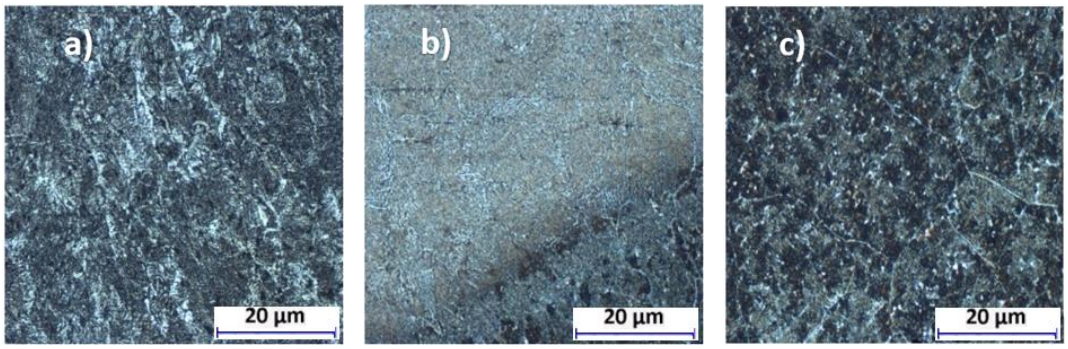

Figure 6. Microstructure of the sample welded using cellulosic electrode by electric arc welding method (100X) (a) SiC without, weld metal, (b) SiC reinforced, HAZ, (c) SiC reinforced weld metal microstructure

In the microstructure of the MAG welded sample, it can be seen that as the ratio of elements such as C and Mn in the welding filler wire increases, the perlite ratio in the microstructure increases and the grains become quite coarse (Figure 7). The intragranular microstructure consists of very fine acicular ferrite. In MAG welding without SiC reinforcement, the desired microstructure is approximately 95% acicular ferrite.

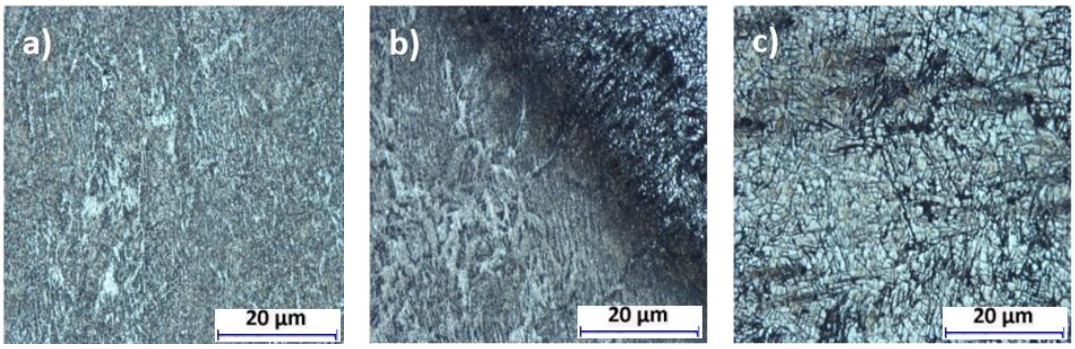

Figure 7. Microstructure of the sample welded by MAG welding method (100X) (a) SiC without, weld metal, (b) SiC reinforced, HAZ, (c) SiC reinforced weld metal microstructure

4. CONCLUSION

In this study, it was observed that the cooling time in the welding area and the carbon and other alloying elements in the additional wire content affected the phase amounts and grain structure change, and also affected the mechanical test results. A needle and oriented epitaxial microstructure was formed in the suddenly cooled region. It was observed that the mechanical properties of samples welded with oxy-gas were the lowest compared to other applied welding methods. When EAW, which is performed with lower heat input, is compared to welds made using the oxy-gas welding method, it is seen that the intragranular structures become thinner.

It was observed that the mechanical properties of SiC reinforced samples improved compared to the samples without SiC reinforcement. It has been determined that SiC reinforcement significantly increases the hardness values of the weld zone.

5. CONFLICT OF INTEREST

Authors approve that to the best of their knowledge, there is not any conflict of interest or common interest with an institution/organization or a person that may affect the review process of the paper.

6. AUTHOR CONTRIBUTION

Rıza KARA, Fatih ÇOLAK and Gökhan YILDIRIM determining the concept and design process of the research and research management, Hakan Furkan AKSU data collection and analysis, Rıza KARA and Fatih ÇOLAK data analysis and interpretation of results.

7. REFERENCES

Abedi S. S., Abdolmaleki A., Adibi N., Failure analysis of SCC and SRB induced cracking of a transmission oil products pipeline. Engineering Failure Analysis, 14(1), 250–261, 2007.

API specification 5L, Specification for line pipe, 46th Edition, USA, 2018.

Baek J., Hyun K., Pyo Y., Kim C., Man K., W. Sik S., Sung C., Effects of pre-strain on the mechanical properties of API 5L X65 pipe. Materials Science and Engineering A, 527(6), 1473–1479, 2010.

Bhadeshia H. K. D. H., Developments in martensitic and bainitic steels: role of the shape deformation. Materials Science and Engineering: A, 378(1–2), 34–39, 2004.

Biresselioglu M. E., Yelkenci T., Oz I. O., Investigating the natural gas supply security: A new

perspective. Energy, 80, 168–176, 2015.

Bohemen S. M.,Van C., Morsdorf L., Acta Materialia Predicting the M s temperature of steels with a thermodynamic based model including the effect of the prior austenite grain size. Acta Materialia, 125, 401–415, 2017.

Candan İ., Durgutlu A., Kahraman N., Gülenç B., Farklı Pozisyonlarda MAG Kaynağı ile Birleştirilen Boruların Kaynak Dikişlerinin Ultrasonik ve Mekanik Muayenesi. Politeknik Dergisi, 2006.

Capelle J., Dmytrakh I., Azari Z., Pluvinage G., Evaluation of electrochemical hydrogen absorption in welded pipe with steel API X52. International Journal of Hydrogen Energy, 38(33), 14356–14363, 2013.

Ezer M., Cam, G., A Study on microstructure and mechanical performance of gas metal arc welded AISI 304L joints. Materialwissenschaft und Werkstofftechnik, 53 (9), 1043-1052, 2022.

Ghosh C., Basabe V. V., Jonas J. J., Kim Y., Jung I.-H., Yue S., The dynamic transformation of deformed austenite at temperatures above the Ae 3. Acta Materialia, 61(7), 2348–2362, 2013.

Handoko W., Pahlevani F., Hossain R., Sahajwalla V., Stress-induced phase transformation and its correlation with corrosion properties of dual-phase high carbon steel. Journal of Manufacturing and Materials Processing, 3(3), 2019.

Hossain R., Pahlevani F., Sahajwalla V., Effect of small addition of Cr on stability of retained austenite in high carbon steel. Materials Characterization, 125, 114–122, 2017.

Hossain R., Pahlevani F., Sahajwalla V., Stability of retained austenite in high carbon steel – Effect of post-tempering heat treatment. Materials Characterization, 149(November 2018), 239–247, 2019.

Iseki T., Kameda T., Maruyama T., Interfacial reactions between SiC and aluminium during joining. Journal of Materials Science, 19, 1984.

Javidi M., Bahalaou H. S., Investigating the mechanism of stress corrosion cracking in near-neutral and high pH environments for API 5L X52 steel. Corrosion Science, 80, 213–220, 2014.

Jayashree P. K., Gowrishankar M. C., Sharma S., Shetty R., Shettar M., Hiremath P., Influence of homogenization and aging on tensile strength and fracture behavior of TIG welded Al6061-SiC composites. Journal of Materials Research and Technology, 9(3), 3598–3613, 2020.

Jonas J. J., Ghosh C., Role of mechanical activation in the dynamic transformation of austenite. Acta Materialia, 61(16), 6125–6131, 2013.

Ju J. B., Lee J. S., Jang J. I., Kim W. S., Kwon D., Determination of welding residual stress distribution in API X65 pipeline using a modified magnetic Barkhausen noise method. International Journal of Pressure Vessels and Piping, 80(9), 641–646, 2003.

Mulder G., Hetland J., Lenaers G., Towards a sustainable hydrogen economy: Hydrogen pathways and infrastructure. International Journal of Hydrogen Energy, 32(10–11), 1324–1331, 2007.

Pk J., Gowrishankar M. C., Sharma S., Shetty R., Hiremath P., Shettar M., The effect of SiC content in aluminum-based metal matrix composites on the microstructure and mechanical properties of welded joints. Journal of Materials Research and Technology, 12, 2325–2339, 2021.

Senol M., Cam G., Investigation into microstructures and properties of AISI 430 ferritic steel butt joints fabricated by GMAW. International Journal of Pressure Vessels and Piping, 202, 104926, 2023.

Serindag H.T., Cam G., Microstructure and mechanical properties of gas metal arc welded AISI 430/AISI 304 dissimilar stainless steels butt joints. Journal of Physics: Conference Series, 1777, 012047, 2021.

Serindag H.T., Cam G., Multi-pass butt welding of thick AISI 316L plates by gas tungsten arc welding: Microstructural and mechanical characterization. International Journal of Pressure Vessels and Piping, 200, 104842, 2022.

Serindag H.T., Tardu C., Kircicek I.O, Cam G., A study on microstructural and mechanical properties of gas tungsten arc welded thick cryogenic 9% Ni alloy steel butt joint. CIRP Journal of Manufacturing Science and Technology, 37, 1-10, 2022.

Serindag H.T., Kircicek I.O, Tardu C., Cam G., Determination of microstructural and mechanical properties of gas tungsten arc welded 9Ni cryogenic steel joint, Mühendis ve Makine (Engineer and Machinery), 63(706), 117-137, 2022.

Serindag H.T., Cam G., Characterizations of microstructure and properties of dissimilar AISI 316L/9Ni low alloy cryogenic steel joints fabricated by GTAW. Journal of Materials Engineering and Performance, 32, 7039-7049, 2023.

Seyedrezai H., Pilkey A. K., Boyd J. D., Effect of pre-IC annealing treatments on the final microstructure and work hardening behavior of a dual-phase steel. Materials Science and Engineering A, 594, 178–188,2014.

Tobón C., Cruz A. M. D., Velázquez J. L. G., Salcedo J. G. G., Salinas R. M., Comparative study on rate of flow accelerated corrosion (FAC) of API 5L X-52-65-70 steels in a brine added with H2S at 60°C by using a rotating cylinder electrode (RCE). International Journal of Electrochemical Science 9 (12): 6781–92, 2014.

Vargas-Arista B., Balvantin A., Baltazar A., García-Vázquez F., On the use of ultrasonic spectral analysis for the characterization of artificially degraded API 5L X52 steel pipeline welded joints. Materials Science and Engineering A, 550, 227–234, 2012.